Superconductivity, metal-insulator transitions and strong enhancement and reduction of isotope effects in the anharmonic Peierls-Hubbard model

1992 J. Phys.: Condens. Matter 4 3793

(http://iopscience.iop.org/0953-8984/4/14/011)

J. Phys.: Condens. Matter 4 (1992) 3793–3811. Printed in the UK

Superconductivity, metal–insulator transitions and strong enhancement and reduction of isotope effects in the anharmonic Peierls–Hubbard model

Keiichiro Nasu

Institute for Molecular Science, Graduate University for Advanced Studies, 38 Nishigo-naka, Myodaiji, Okazaki 444, Japan

Received 16 September 1991, in final form 12 November 1991

Abstract. A quasi-two-dimensional Peierls–Hubbard model with the typical two types of anharmonic phonons has been studied, so as to clarify both the enhancement and reduction of isotope shifts of superconducting (SP) transition temperature T_c, as well as the competition between the metallic state and the charge-density-wave (CDW) or spin-density-wave (SDW) state. The first type is a sextic anharmonicity like a hard-core repulsion, and the second type is a small negative quartic anharmonicity in addition to the sextic one, just like a mixture of a hard core and a soft one. This theory is based on the mean-field approximation for electrons and a variational method for phonons. In the first type, the Peierls distortion is excessively suppressed, and the SP state becomes more stable than the CDW, even when electron–phonon (e–ph) coupling is very strong. Thus, T_c of this case is enhanced, but has no isotope effect. In the second type, in contrast, the SP state is suppressed by the CDW when e–ph coupling is strong. The T_c of this case is reduced, but shows a strongly enhanced isotope shift. In both cases, the SDW is always suppressed.

1. Introduction

Theoretical problems related to strong electron–phonon (e–ph) coupling in conductive crystals have been the subject of considerable interest in recent years. As is well known, e–ph coupling results in a phonon-mediated attraction between electrons. When this attraction is sufficiently strong, the Pauli paramagnetic metallic (PPM) state of electrons becomes unstable, and falls into the charge-density-wave (CDW) state or the superconducting (SP) state, at low temperatures.

In the CDW state, frozen phonons or frozen local lattice distortions appear everywhere in the crystal; each traps two electrons together through e–ph coupling, and finally produces a new spatial order among them. This is one of the well known Peierls-type metal–insulator transitions. On the other hand, in the SP state, we have no frozen phonon, but moving ones that travel together with the conducting electrons, as if they were their 'dresses'. This dressing effect makes electrons paired through e–ph coupling.

These two states are always competing with each other as the ground state of a many-electron system coupling strongly with phonons. This competition is nothing but a competition between the adiabatic nature and the inverse-adiabatic nature of e–ph coupling [1]. In the case of CDW, the electrons follow the frozen local lattice distortions.

On the contrary, in the case of the SP state, the phonons or the local lattice distortions follow the electrons.

Between two electrons, there is also a coulombic repulsion acting, which is always competing with this phonon-mediated attraction. If this repulsion is sufficiently strong, the PPM falls into the spin-density-wave (SDW) state. This is another metal–insulator transition.

These problems related to the competition between the SP state, the CDW state and the SDW state have been the subject of considerable interest in recent years, and various theoretical studies have already been devoted to them [1, 2]. However, in most of these studies, the phonons or the lattice vibrations are tacitly assumed to be perfectly harmonic, although large-amplitude vibrations induced by the strong e–ph coupling will inevitably involve anharmonicities. The so-called 'harmonic approximation', on which we conventionally rely, should not be overrated in the case of strong e–ph coupling, since it is but one possible 'approximation'.

For this reason, in the present paper, we will be concerned with the effects of anharmonicity on the aforementioned competition in the ground state. We will also be concerned with its effect on both the enhancement and reduction of isotope shifts of the superconducting transition temperature T_c.

There may be various types of anharmonicities, for example, one of the double-well types, which results in some specific low-energy phonon modes [3, 4]. However, as is well known, low-energy modes often result in the CDW when they couple with electrons strongly, and finally spoil the SP state. For this reason, throughout this paper, we mainly deal with a local sextic anharmonicity. It causes the potential for the lattice motion to be like a strong inter-ionic repulsion, free from the occurrence of any specific low-energy modes.

These problems are closely related with high-temperature superconductivity of transition-metal oxides [4]. There are various experimental facts that suggest the importance of e–ph coupling in these compounds, for example, the infrared and Raman spectra [5–7], the photo-induced absorption phenomena [8, 9], the tunnelling spectra [10, 11], the T_c degradation due to the structural changes [12–14] and so on. As for the isotopic shift of T_c itself, it is believed to be very small [4]. However, recent experimental studies have clearly shown that there are new cases with enhanced isotope shifts, in addition to the well known cases with reduced shifts [12].

Keeping these problems in mind, in the following sections, we will calculate the phase diagram of a quasi-two-dimensional Peierls–Hubbard model with anharmonic phonons, together with the strong enhancement and reduction of isotope shifts.

2. Quasi-two-dimensional anharmonic Peierls–Hubbard model

Let us start from the following model Hamiltonian ($\equiv H$) for a system composed of N ($\gg 1$) quasi-two-dimensional lattice sites and N electrons, coupling strongly with anharmonic phonons. It is given as

$$H = -\sum_{l,l',\sigma} T(l-l')a_{l\sigma}^{+}a_{l'\sigma} + U\sum_{l}(n_{l\alpha}-\bar{n})(n_{l\beta}-\bar{n}) - S\sum_{l,\sigma}Q_l(n_{l\sigma}-\bar{n})$$
$$+\sum_{l}\left(\frac{P_l^2}{2M}+\frac{K}{2}Q_l^2-\frac{B}{2}Q_l^4+\frac{C}{2}Q_l^6\right) \qquad n_{l\sigma}\equiv a_{l\sigma}^{+}a_{l\sigma}. \tag{2.1}$$

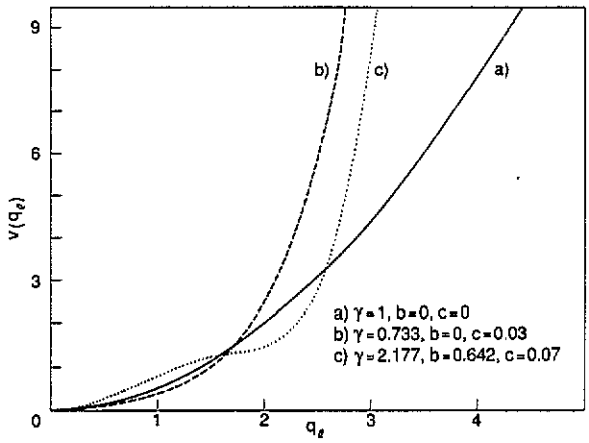

Figure 1. Plots of $v(q_l)$ as a function of q_l. The full curve denotes the harmonic case. The broken curve is the hard-core case. The dotted curve is the mixed case.

Here, $T(l-l')$ is the transfer energy of an electron between two sites l and l' in a quasi-two-dimensional square lattice; $a_{l\sigma}^{+}$ is the creation operator of an electron at site l with spin σ ($=\alpha$ or β); U is the Hubbard-type coulombic repulsive energy; $\bar{n}$ ($=0.5$) is half of the average electron number; S is the coupling constant between the electron and phonon localized at site l; Q_l is the coordinate of this phonon mode and P_l is its conjugate momentum; M denotes the effective mass for this mode; K (>0) is the harmonic spring constant, with positive value; B (≥ 0) and C (>0) denote the constants of quartic and sextic anharmonicities, respectively.

In practical calculations, we assume that the full width of the electron energy band is about 2 eV, and the phonon energy is about 0.08 eV. This is a standard case widely realized in transition-metal oxides, when the electron is coupling with the breathing motion of oxygen.

We also assume that $T(l-l')$ between nearest-neighbour sites of the square lattice is T, while that between next-nearest-neighbour sites is $0.35\,T$. As shown in our previous paper, this set of transfer energies gives an almost circular Fermi surface, and the nesting-type instability does not occur when the e–ph coupling is weak [1]. Hence, transitions from a metal to insulators can occur only in the strong region of e–ph coupling, and we can focus our attention only on these regions.

As for the anharmonicity, we have assumed the sextic one with no or a small negative quartic one, as shown in figure 1. It makes the potential for the quantum motion of the lattice like a strong inter-ionic repulsion. Contrary to the case of a double well, the harmonic spring constant K is also assumed to be positive, and hence we have no specific low-energy phonon mode [3]. Thus, the possibility of lattice instabilities has been excluded in the case of weak e–ph coupling.

Using this anharmonic model, we will also study the isotope effect on the SP state. For this reason, we now introduce a harmonic phonon with a spring constant ($\equiv K_0$) and a mass ($\equiv M_0$), which hereafter act as a reference for various anharmonic cases. In terms of these K_0 and M_0, we can also define a reference phonon energy ($\equiv \hbar\omega_0$), which is given as

$$\omega_0 \equiv (K_0/M_0)^{1/2}. \tag{2.2}$$

Taking this $\hbar\omega_0$ as the unit of energy, we transform all the quantities into dimensionless form as

$$q_l \equiv (M_0\omega_0/\hbar)^{1/2}Q_l \qquad p_l \equiv P_l/(\hbar M_0\omega_0)^{1/2} \tag{2.3}$$

$$h \equiv H/\hbar\omega_0 \qquad t(l-l') \equiv T(l-l')/\hbar\omega_0 \qquad t \equiv T/\hbar\omega_0$$
$$u \equiv U/\hbar\omega_0 \qquad s \equiv S^2/M_0\hbar\omega_0^3 \qquad b \equiv \hbar B/M_0^2\omega_0^3 \tag{2.4}$$
$$c \equiv \hbar^2 C/M_0^3\omega_0^4 \qquad \Delta \equiv M/M_0 - 1 \qquad \gamma \equiv K/K_0.$$

In terms of these dimensionless quantities, the new Hamiltonian h can be written as

$$h = -\sum_{l,l',\sigma} t(l-l')a_{l\sigma}^{+}a_{l'\sigma} + u\sum_{l}(n_{l\alpha}-\bar{n})(n_{l\beta}-\bar{n}) - s^{1/2}\sum_{l,\sigma} q_l(n_{l\sigma}-\bar{n})$$
$$+ \sum_{l}\left(\frac{p_l^2}{2(1+\Delta)} + v(q_l)\right) \qquad v(q_l) \equiv (\gamma q_l^2 - bq_l^4 + cq_l^6)/2. \tag{2.5}$$

Here $v(q_l)$ denotes the potential for lattice motion with a local anharmonicity. Its jth eigenvalue ($\equiv\varepsilon_j$) and eigenfunction ($\equiv|j, l\rangle$) at site l are determined from the following equation:

$$\left(p_l^2/2(1+\Delta) + v(q_l)\right)|j, l(\Delta,\gamma,b,c)\rangle \equiv \varepsilon_j(\Delta,\gamma,b,c)\,|j, l(\Delta,\gamma,b,c)\rangle$$
$$j = 0, 1, 2, \ldots. \tag{2.6}$$

Various anharmonic vibrations will appear as a function of γ, b and c. However, as mentioned before, we are interested only in a quite standard case of vibration, in the sense that this anharmonicity results in neither a specific low-energy mode nor a specific high-energy one. In order to focus our attention only on such a standard case, we use some selected values for γ. That is, we change the value of γ from 1 as c increases from 0, so that the lowest vibrational excitation energy remains unchanged in spite of the anharmonicity. This condition is written as

$$\varepsilon_{10}(0,\gamma,b,c) = \varepsilon_{10}(0,1,0,0) = 1 \tag{2.7}$$

where

$$\varepsilon_{jj'}(\Delta,\gamma,b,c) \equiv \varepsilon_j(\Delta,\gamma,b,c) - \varepsilon_{j'}(\Delta,\gamma,b,c). \tag{2.8}$$

As for b, we take two typical cases with zero or a small negative quartic anharmonicity, that is, $b = 0$ or $b = 9.17c$. For these two cases, γ, ε_{10} and ε_{20} are determined from equations (2.7) and (2.6) as functions of c, and are shown in figures 2 and 3, while examples of $v(q_l)$ for these cases are shown in figure 1.

Let us see why these two cases are typical and important, in connection with strong enhancement and reduction of isotopic shifts. The Bardeen–Cooper–Schrieffer (BCS) theory tells us that e–ph coupling in equation (2.5) results in an inter-electron attraction

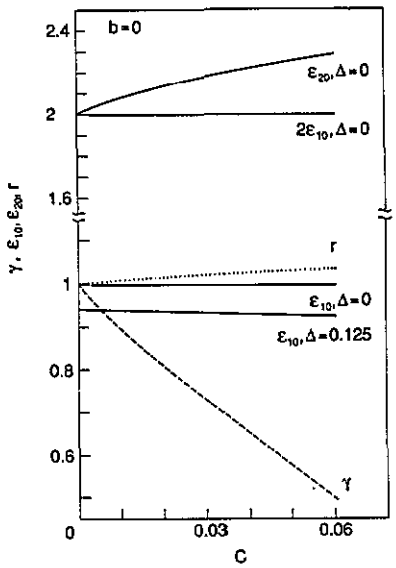

Figure 2. Plots of γ, ε_{10} $(0, \gamma, b, c)$, $\varepsilon_{10}(0.125, \gamma, b, c)$, $\varepsilon_{20}(0, \gamma, b, c)$ and r as functions of c, for $b = 0$.

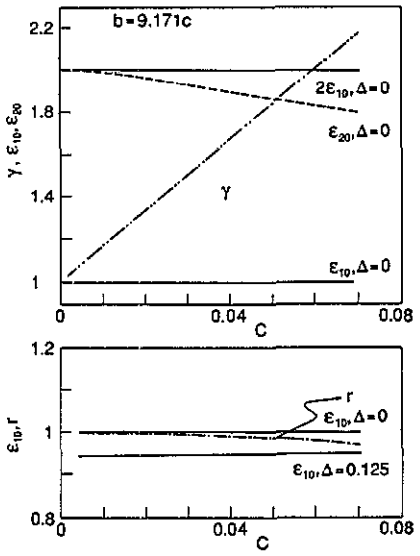

Figure 3. Plots of $\gamma, \varepsilon_{10}(0, \gamma, b, c)$, $\varepsilon_{10}(0.125, \gamma, b, c)$, $\varepsilon_{20}(0, \gamma, b, c)$ and r as functions of c, for $b = 9.171c$.

only within a narrow energy region around the Fermi level. The energy width of this attractive region is nothing but

$$\varepsilon_{10} \tag{2.9}$$

while the strength of attraction ($\equiv F_{\text{eff}}$) is given as

$$F_{\text{eff}} = s \sum_{l} N^{-1} |\langle 1l|q_l|0l\rangle|^2/\varepsilon_{10}. \tag{2.10}$$

It has the transition matrix element $|\langle 1l|q_l|0l\rangle|^2$ in its numerator.

In terms of these ε_{10}, $|\langle 1l|q_l|0l\rangle|^2$ and F_{eff}, we can easily understand the relation between isotope shifts and anharmonicities qualitatively. In the harmonic case, $|\langle 1l|q_l|0l\rangle|^2$ and ε_{10} decrease in entirely the same way as Δ increases. Hence, F_{eff} in equation (2.10) becomes independent of Δ, and only the attractive region (2.9) decreases according to the increase of Δ, as schematically shown (figure 4(a)). This is the well known logic of why we get the normal isotope shift.

Anharmonicities change this relation greatly. One example for the extremely anharmonic case is the hard-core repulsion with an infinite barrier shown in figure 4(b). In this case, the vibronic wavefunctions $|j, l\rangle$ ($j = 0, 1, \ldots$) are independent of Δ, being determined only by the boundary condition at the hard core, while ε_{10} always decreases as Δ increases, and hence F_{eff} in equation (2.10) increases as Δ increases, as shown in figure 4(b). Thus, the increase of the attraction and the decrease of the attractive region compete with each other, resulting in only a small or zero isotope shift. In some cases, it will give even negative ones. The case with $b = 0$ corresponds to this hard-core case, and the nature of $v(q_l)$ of this case is shown by the broken curve in figure 1.

We can also think of a mixture of a hard core and a soft one, with a step in its $v(q_l)$, as schematically shown in figure 4(c). In this case, the wavefunction of lowest state $|0, l\rangle$,

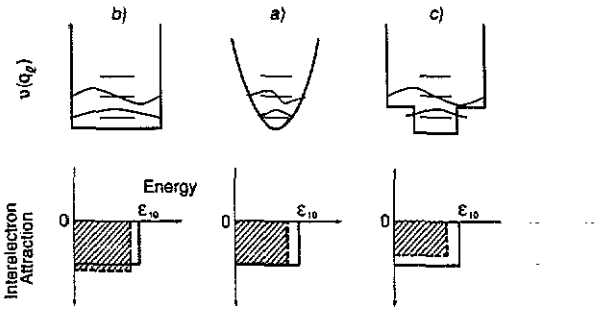

Figure 4. Schematic nature of $v(q_l)$ and inter-electron attraction: (*a*) harmonic case; (*b*) hard-core case; (*c*) mixed case. The upper figures denote $v(q_l)$ together with the vibronic wavefunctions. The lower figures denote the inter-electron attraction as functions of energy from the Fermi level. The broken lines and shaded area denote the attraction after isotopic substitution.

being localized strongly within the lower well, shrinks much more rapidly than the excited state $|1, l\rangle$ as Δ increases. This state $|1, l\rangle$ is almost independent of Δ, for the same reason as mentioned before. Hence, the decrease of the matrix element $|\langle 1l|q_l|0l\rangle|^2$ becomes greater than that of ε_{10}. Consequently, both F_{eff} and the attractive region decrease as Δ increases. This situation is schematically shown in figure 4(*c*). Thus, the isotope effect will be strongly enhanced, and this is the case corresponding to $b = 9.17c$. In this case $v(q_l)$ is also shown by the dotted curve in figure 1, and it has a region that looks like a plateau at around $q_l = 1.5$.

Exactly speaking, however, in both these two anharmonic cases, $v(q_l)$ is a monotonically increasing function of $|q_l|$ ($\neq 0$).

Finally, it should be noted that our way of thinking in the present paper is quite phenomenological, in the sense that we will not be concerned with the microscopic origin of the anharmonicity. From this point of view, in the next sections, we will calculate its effects on the metal–insulator transitions, T_c and its isotope shifts in detail.

3. Charge-density-wave state

Using γ, b and c, thus selected, we will calculate here the energy of the CDW state. In this state, as mentioned before, frozen phonons or frozen local lattice distortions appear everywhere in the crystal, each of which traps two electrons together, and finally produces a spatial order among them. Since the lattice has a quantum nature, it still oscillates around this distorted position. However, because of the anharmonicity, the width of this quantum oscillation will also be greatly changed from that of the aforementioned reference state with $\gamma = 1$ and $b = c = 0$.

In order to take these two effects into account, we introduce the following two transformations for phonons. The first is the transformation ($\equiv M_f$) that generates the frozen distortion. It is given as

$$M_f = \exp\left(- \mathrm{i} s^{1/2} \sum_l \overline{q_l} p_l \right) \tag{3.1}$$

where $\overline{q_l}$ denotes the displacement of the equilibrium position of the phonon at site l, as clearly seen below:

$$M_f^{-1} q_l M_f = q_l + s^{1/2} \overline{q_l}. \tag{3.2}$$

The second is the so-called scaling transformation ($\equiv M_s$), which changes the width of the quantum oscillation from that of the reference one. It is given as

$$M_s = \exp\left(\frac{i}{4}\sum_l \ln \lambda_l (p_l q_l + q_l p_l)\right). \tag{3.3}$$

Here λ_l (>0) is the scaling parameter. It decreases or increases the width of oscillation as it becomes smaller or bigger than 1, respectively. This effect can be easily seen from the following results:

$$M_s^{-1} q_l M_s = \lambda_l^{1/2} q_l \qquad M_s^{-1} p_l M_s = \lambda_l^{-1/2} p_l. \tag{3.4}$$

These parameters, $\overline{q_l}$ and λ_l, are unknown at present, and should be determined later within a variational method. By these M_f and M_s, h is transformed as

$$\begin{aligned} M_s^{-1} M_f^{-1} h M_f M_s = &- \sum_{l,l',\sigma} t(l-l') a_{l\sigma}^{+} a_{l'\sigma} + u \sum_l (n_{l\alpha} - \bar{n})(n_{l\beta} - \bar{n}) \\ &- s^{1/2} \sum_{l,\sigma} (\lambda_l^{1/2} q_l + s^{1/2} \overline{q_l})(n_{l\sigma} - \bar{n}) \\ &+ \sum_l \left(\frac{p_l^2}{2(1+\Delta)\lambda_l} + v(\lambda_l^{1/2} q_l + s^{1/2} \overline{q_l})\right). \end{aligned} \tag{3.5}$$

We now calculate the ground state ($\equiv |g\rangle\!\rangle$) of this transformed Hamiltonian $M_s^{-1} M_f^{-1} h M_f M_s$, within the mean-field theory for inter-electron interactions and by a variational method for phonons. Since both the displacement of the equilibrium position and the change of oscillation width have already been taken into account, we make the approximation that the phonon part of $|g\rangle\!\rangle$ is the aforementioned reference state. Then we can write $|g\rangle\!\rangle$ as

$$|g\rangle\!\rangle = |g)) \prod_l |0, l(0,1,0,0)\rangle \tag{3.6}$$

where $|g))$ denotes the electronic part of the ground state. At the present stage, this $|g))$ is unknown and should be determined later self-consistently within the mean-field theory. Taking the average with respect to the reference state of the phonon, we can get a reduced Hamiltonian for the electrons alone as

$$\begin{aligned} \langle M_s^{-1} M_f^{-1} h M_f M_s \rangle = &- \sum_{l,l',\sigma} t(l-l') a_{l\sigma}^{+} a_{l'\sigma} + u \sum_l (n_{l\alpha} - \bar{n})(n_{l\beta} - \bar{n}) - s \sum_{l,\sigma} \overline{q_l}(n_{l\sigma} - \bar{n}) \\ &+ \sum_l \left(\frac{1}{4(1+\Delta)\lambda_l} + \frac{\gamma}{4}(\lambda_l + 2s\overline{q_l^2}) - \frac{b}{8}(3\lambda_l^2 + 12s\lambda_l \overline{q_l^2} + 4s^2 \overline{q_l^4}) \right. \\ &\left. + \frac{c}{16}(11\lambda_l^3 + 90s\lambda_l^2 \overline{q_l^2} + 60\lambda_l s^2 \overline{q_l^4} + 8s^3 \overline{q_l^6})\right) \end{aligned} \tag{3.7}$$

where $\langle \ldots \rangle$ is defined as

$$\langle \ldots \rangle \equiv \prod_l \langle 0, l(0,1,0,0)| \ldots |0, l(0,1,0,0)\rangle \tag{3.8}$$

and in this calculation we have also used the relations

$$\langle p_l^2 \rangle = \langle q_l^2 \rangle = 1/2 \qquad \langle q_l^4 \rangle = 3/4 \qquad \langle q_l^6 \rangle = 11/8.$$

Again taking the average of this reduced Hamiltonian with respect to the electronic part $|g)$, we can formally obtain the total energy of our system as

$$((\langle M_s^{-1}M_f^{-1}hM_fM_s\rangle)) \qquad ((\ldots)) \equiv ((g|\ldots|g)). \tag{3.9}$$

From this result, $\overline{q_l}$ can be determined by the condition of energy minimization, i.e.

$$\partial((\langle M_s^{-1}M_f^{-1}hM_fM_s\rangle))/\partial\overline{q_l} = 0 .$$

and it gives the following equation for $\overline{q_l}$:

$$\sum_\sigma [((n_{l\sigma})) - \bar{n}] = \overline{q_l}[\gamma - b(3\lambda_l + 2s\overline{q_l^2}) + \tfrac{3}{4}c(15\lambda_l^2 + 20\lambda_l s\overline{q_l^2} + 4s^2\overline{q_l^4})]. \tag{3.10}$$

On the other hand, the condition of energy minimization with respect to λ_l,

$$\partial((\langle M_s^{-1}M_f^{-1}hM_fM_s\rangle))/\partial\lambda_l = 0$$

gives the following equation for λ_l:

$$1/[(1+\Delta)\lambda_l^2] = \gamma - 3b(\lambda_l + 2s\overline{q_l^2}) + \tfrac{3}{16}c(11\lambda_l^2 + 60\lambda_l s\overline{q_l^2} + 20s^2\overline{q_l^4}). \tag{3.11}$$

In order to determine $|g)$ with the CDW-type broken symmetry, we assume that the electron density $[((n_{l\sigma})) - \bar{n}]$ and $\overline{q_l}$ spatially oscillate with twice the period of the original lattice in both directions of the crystal axes, while λ_l is independent of l as

$$[((n_{l\sigma})) - n] \to \delta n\, e^{iw\cdot l} \qquad \overline{q_l} \to \bar{q}\, e^{iw\cdot l} \qquad \lambda_l \to \lambda \qquad w \equiv (\pi, \pi). \tag{3.12}$$

Here, δn and $\bar{q}$ are the amplitudes of these oscillations, and λ denotes the common scaling parameter. The unit of length is the lattice constant. Within this approximation, the reduced Hamiltonian $\langle M_s^{-1}M_f^{-1}hM_fM_s\rangle$ can be replaced by a mean-field Hamiltonian ($\equiv h_{CDW}$) of the CDW state as

$$\langle M_s^{-1}M_f^{-1}hM_fM_s\rangle \to h_{CDW}$$

and h_{CDW} is given by

$$h_{CDW} = -\sum_{l,l',\sigma} t(l-l')a_{l\sigma}^{+}a_{l'\sigma} - J\sum_{l,\sigma} e^{iw\cdot l}n_{l\sigma} + NL(\delta n, \lambda, \bar{q}) \tag{3.13}$$

with

$$L(\delta n, \lambda, \bar{q}) \equiv -u\delta n^2 + 1/[4(1+\Delta)\lambda] + \tfrac{1}{4}(\gamma + 2s\bar{q}^2) - \tfrac{1}{8}b(3\lambda^2 + 12\lambda s\bar{q}^2 + 4s^2\bar{q}^4)$$
$$+ \tfrac{1}{16}c(11\lambda^3 + 90\lambda^2 s\bar{q}^2 + 60\lambda s^2\bar{q}^4 + 8s^3\bar{q}^6).$$

Here, J in the second term denotes the energy gap due to the CDW-type broken symmetry, and is given as

$$J \equiv (s\bar{q} - u\delta n). \tag{3.14}$$

Using the following Fourier components of $a_{l\sigma}$ and $t(l)$ with a wavevector k,

$$a_{k\sigma} \equiv \sum_l N^{-1/2} e^{-ik\cdot l}a_{l\sigma} \qquad e(k) \equiv \sum_l e^{ik\cdot l}t(l) \tag{3.15}$$

we can rewrite h_{CDW} in a 2×2 matrix form as

$$h_{\mathrm{CDW}} = \sum_{k,\sigma}^{\mathrm{HZ}} [a_{k\sigma}^{+}, a_{k+w,\sigma}^{+}] \begin{bmatrix} -e(k) & -J \\ -J & -e(k+w) \end{bmatrix} \begin{bmatrix} a_{k\sigma} \\ a_{k+w,\sigma} \end{bmatrix} + NL(\delta n, \lambda, \bar{q}). \tag{3.16}$$

Here, HZ of Σ means that the summation over k should be taken within a half of the first Brillouin zone.

This 2×2 matrix can be diagonalized by the following unitary transformation:

$$\begin{bmatrix} Z_{k1\sigma} \\ Z_{k2\sigma} \end{bmatrix} = \begin{bmatrix} \cos(\varphi_k) & \sin(\varphi_k) \\ -\sin(\varphi_k) & \cos(\varphi_k) \end{bmatrix} \begin{bmatrix} a_{k\sigma} \\ a_{k+w,\sigma} \end{bmatrix}$$

$$\varphi_k \equiv \arctan\left(\frac{E(k) - e^{-}(k)}{E(k) + e^{-}(k)}\right)^{1/2} \qquad E(k) \equiv [e^{-}(k)^2 + J^2]^{1/2} \tag{3.17}$$

$$e^{\pm}(k) \equiv [e(k) \pm e(k+w)]/2$$

and we get new Fermion operator $Z_{kio}(i = 1, 2)$ with energy $E_i(k)$ defined as

$$E_i(k) \equiv -e^{+}(k) + (-1)^i E(k) \qquad i = 1, 2. \tag{3.18}$$

We can easily infer that the energy levels with $i = 1$ are below the energy gap, while those with $i = 2$ are above it. From these results, we can get the total energy as

$$((h_{\mathrm{CDW}})) = \sum_{k,\sigma}^{\mathrm{HZ}} \sum_{i=1,2} E_i(k) n(E_i(k) - \mu) + NL(\delta n, \lambda, \bar{q}). \tag{3.19}$$

Here, $n(E)$ is the occupation number of the electron, and μ denotes the chemical potential of this system; $n(E)$ is given as

$$n(E) \equiv (\mathrm{e}^{\theta E} + 1)^{-1} \qquad \theta \equiv \hbar\omega_0 / k_{\mathrm{B}} T_{\mathrm{temp}}$$

and T_{temp} denotes temperature.

The amplitude δn should be determined so as to satisfy equation (3.12). From this condition we get the following self-consistency equation for δn:

$$\delta n = \sum_{k}^{\mathrm{HZ}} \left(\frac{N}{2}\right)^{-1} \frac{D}{2E(k)} [n(E_1(k) - \mu) - n(E_2(k) - \mu)]. \tag{3.20}$$

Solving this equation together with equations (3.10), (3.11) and (3.12), we can finally determine the total energy, δn, $\bar{q}$ and λ, self-consistently.

4. Metallic state and spin-density-wave state

Let us now proceed to the PPM state. In contrast to the CDW, we have no frozen lattice distortion in this state, but have moving lattice distortions that travel from site to site together with the electrons as their 'dresses'. In order to describe this effect, we introduce the following transformation M_{m} that generates this moving distortion:

$$M_{\mathrm{m}} \equiv \exp\left(-\mathrm{i}s^{1/2} q \sum_{l,\sigma} (n_{l\sigma} - \bar{n}) p_l \right). \tag{4.1}$$

Here q is a variational parameter that denotes the thickness of the distortion cloud or the phonon cloud around an electron. By this M_m, q_l is transformed as

$$M_m^{-1} q_l M_m = q_l + s^{1/2} q \sum_\sigma (n_{l\sigma} - \bar{n})$$

and the second term denotes the displacement of the equilibrium position. In contrast to equation (3.2), this displacement appears or disappears according to the presence or absence of electrons at site l, because it is proportional to the electron number operator $(n_{l\sigma} - \bar{n})$. This M_m also transforms the bare electron operator $a_{l\sigma}^+$ into a localized polaron one with a phonon cloud around itself as

$$M_m^{-1} a_{l\sigma}^+ M_m = a_{l\sigma}^+ \exp(-is^{1/2} q p_l). \tag{4.2}$$

This distortion cloud not only moves from site to site, but also oscillates quantum-mechanically within each site. Similar to the case of CDW, the width of this oscillation will be changed from that of the reference state, because of an interplay between the anharmonicity and the e–ph coupling. In order to take these two effects of phonons into account, we transform h as

$$\begin{aligned} M_s^{-1} M_m^{-1} h M_m M_s = &- \sum_{l,l',\sigma} t(l-l') a_{l\sigma}^+ a_{l'\sigma} \exp[-is^{1/2} q (p_l \lambda_l^{-1/2} - p_{l'} \lambda_{l'}^{-1/2})] \\ &+ u \sum_l (n_{l\alpha} - \bar{n})(n_{l\beta} - \bar{n}) \\ &- s^{1/2} \sum_{l,\sigma} \lambda_l^{1/2} q_l (n_{l\sigma} - \bar{n}) - sq \sum_{l,\sigma,\sigma'} (n_{l\sigma'} - \bar{n})(n_{l\sigma} - \bar{n}) \\ &+ \sum_l \left(\frac{p_l^2}{2(1+\Delta)\lambda_l} + v(\lambda_l^{1/2} q_l + s^{1/2} q \sum_\sigma [n_{l\sigma} - \bar{n}]) \right). \end{aligned} \tag{4.3}$$

Here, the first term denotes the transfer of a polaron with a phonon cloud around itself. The third term denotes the coupling between the polaron and the new phonon, whose equilibrium position has already been displaced by M_m. The fourth term denotes the inter-polaron attraction, which also includes the energy lowering due to the self-interaction of an electron, coming from the e–ph coupling.

Within the same approximation for the ground state $|g\rangle\!\rangle$ as described by equation (3.6), we get a reduced Hamiltonian only for the polarons in the PPM state as

$$\begin{aligned} \langle M_s^{-1} M_m^{-1} h M_m M_s \rangle = &- \sum_{l,l',\sigma} t(l-l') a_{l\sigma}^+ a_{l'\sigma} \exp[-\tfrac{1}{4} sq^2 (\lambda_l^{-1} + \lambda_{l'}^{-1})] \\ &+ \sum_l \{u - sq[2 - \gamma q + b(3q\lambda_l + sq^3) \\ &- \tfrac{1}{4} cq(45\lambda_l^2 + 30\lambda_l sq^2 + 4s^2 q^4)]\}(n_{l\alpha} - \bar{n})(n_{l\beta} - \bar{n}) \\ &+ \sum_l \left(\frac{1}{(1+\Delta)\lambda_l} + \lambda_l [\gamma - \tfrac{3}{2} b(\lambda_l + 2sq^2) + \tfrac{1}{4} c(11\lambda_l^2 + 45\lambda_l sq^2 \right. \\ &\left. + 30s^2 q^4)] \right) \Big/ 4 - sqN(2 - q\gamma + bsq^3 - cs^2 q^5)/4 \end{aligned} \tag{4.4}$$

and in this calculation, we have used the following equality:

$$\left(\sum_{\sigma}(n_{l\sigma}-\bar{n})\right)^{2i}=2(n_{l\alpha}-\bar{n})(n_{l\beta}-\bar{n})+1/2 \qquad i=1,2,\ldots. \tag{4.5}$$

The first term of equation (4.4) denotes the effective transfer of a polaron, with the reduction factor exp(...) coming from the overlap integral between the two phonon clouds at sites l and l'. The second term denotes the interactions between two polarons with opposite spins to each other. The fourth and the third terms denote the energy lowering due to the aforementioned self-interaction, the interplay between the anharmonicity and the e–ph coupling, and the quantum oscillation energies of phonons.

Since we are going to calculate the total energy of the PPM state within the mean-field theory, we approximate the scaling parameter and the average electron density as

$$\lambda_l \to \lambda \qquad [((n_{l\sigma}))-\bar{n}] \to 0.$$

Thus, we can formally describe the total energy of the PPM state in the following form:

$$\begin{aligned}(((\langle M_{\mathrm{s}}^{-1}M_{\mathrm{m}}^{-1}hM_{\mathrm{m}}M_{\mathrm{s}}\rangle))) &= -2\exp(-sq^2/2\lambda)\sum_{k}e(k)n(-e(k)-\mu)\\ &+N\left(-\frac{sq}{2}+\frac{1}{4(1+\Delta)\lambda}+\frac{\gamma(\lambda+sq^2)}{4}-\frac{b}{8}(3\lambda^2+6\lambda sq^2+2s^2q^4)\right.\\ &\left.+\frac{c}{16}(11\lambda^3+45\lambda^2sq^2+30\lambda s^2q^4+4s^3q^6)\right)\end{aligned} \tag{4.6}$$

where μ denotes the chemical potential of the non-interacting electron system.

The thickness of the phonon cloud q can be determined by the condition of energy minimization,

$$\partial(((\langle M_{\mathrm{s}}^{-1}M_{\mathrm{m}}^{-1}hM_{\mathrm{m}}M_{\mathrm{s}}\rangle)))/\partial q=0$$

and we get the equation for q as

$$\begin{aligned}q=\Bigg[&\gamma-b(3\lambda+2sq^2)+\frac{3c}{4}(15\lambda^2+20\lambda sq^2+4s^2q^4)\\ &+\frac{4}{\lambda}\exp\left(-\frac{sq^2}{2\lambda}\right)\sum_{k}N^{-1}e(k)n(-e(k)-\mu)\Bigg]^{-1}.\end{aligned} \tag{4.7}$$

The condition of energy minimization with respect to λ,

$$\partial(((\langle M_{\mathrm{s}}^{-1}M_{\mathrm{m}}^{-1}hM_{\mathrm{m}}M_{\mathrm{s}}\rangle)))/\partial\lambda=0$$

gives the equation for λ as

$$\begin{aligned}&\tfrac{33}{4}c\lambda^4+(\tfrac{99}{4}csq^2-3b)\lambda^3+(\tfrac{39}{4}cs^2q^4+\gamma-3bsq^2)\lambda^2\\ &\quad=\frac{1}{(1+\Delta)}+4sq^2\exp\left(-\frac{sq^2}{2\lambda}\right)\sum_{k}N^{-1}e(k)n(-e(k)-\mu).\end{aligned} \tag{4.8}$$

From these equations, we can finally determine the total energy, q and λ.

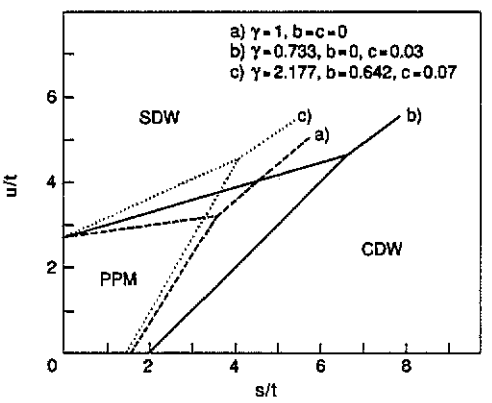

Figure 5. The phase diagram as a function of u/t and s/t, for $t = 3.125$. The broken lines denote the harmonic case, $\Delta = 0$, $\gamma = 1$ and $b = c = 0$.

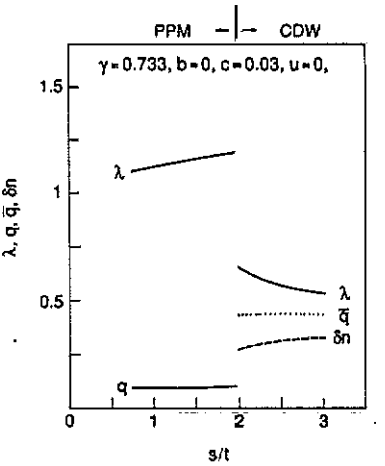

Figure 6. Plots of λ, q, $\bar{q}$ and δn as functions of s/t, for $u = 0$, $t = 3.125$.

Let us now proceed to the SDW state. In the case of SDW, the calculation is almost the same as the previous two cases, except that the phases of the electron density oscillations are opposite between the spin-up electrons and the spin-down ones, and also the frozen distortion is absent, as

$$[((n_{l\alpha})) - \bar{n}] \rightarrow \delta n\, e^{iw \cdot l} \qquad [((n_{l\beta})) - \bar{n}] \rightarrow -\delta n\, e^{iw \cdot l} \qquad \overline{q_l} = 0. \tag{4.9}$$

It will not be necessary for us to repeat them again in detail.

5. Phase diagram and anharmonicity

From the results obtained in previous sections, we can complete the phase diagram of our system at absolute zero temperature. As one of its typical results, we fix t at $t = 3.125$ so as to make the full electron bandwidth 2 eV, and describe the phase diagram in a two-dimensional space spanned by u/t and s/t, as shown in figure 5. Since the Fermi surface of a non-interacting electron is a circle with no nesting, we have the PPM state in the region of small u and s, while the SDW appears in the large u region, and the CDW appears in the large s region.

The broken lines denote the phase boundary of the reference phonon state with $\Delta = 0$, $b = c = 0$ and $\gamma = 1$. When $u/t = 0$, the transition from the PPM to the CDW occurs at around $s/t = 1.6$, while when $s/t = 0$, the transition from the PPM to the SDW occurs at around $u/t = 2.7$.

In the case of the hard-core type anharmonicity with $\gamma = 0.733$, $b = 0$ and $c = 0.03$, the PPM remains more stable than the CDW in much stronger regions of s/t than the previous harmonic case, as seen from the full lines. Even the SDW state is also seen to be suppressed by this anharmonicity, since the PPM region also expands into a new region of stronger u. This suppression of CDW relative to the PPM can be understood straight away from the broken curve in figure 1. A large-amplitude Peierls distortion is greatly suppressed, because of the non-linear increase of the potential energy $v(q_l)$.

Figure 6 shows the changes of λ, q, $\bar{q}$ and δn as functions of s/t along the line $u/t = 0$. In the PPM region, λ is almost the same as that of the reference state, $\lambda \simeq 1$, and q is also very small as expected from Migdal's theorem, $q \simeq 0.1$. Both of them increase as s/t comes close to the phase boundary. As s/t exceeds 1.97, however, δn and $\bar{q}$ become finite, and λ decreases down to about 0.6. This sudden decrease of λ is due to the increase of the curvature of the potential energy surface around the new equilibrium position of the lattice.

We have already shown that the PPM erodes even the SDW in the anharmonic case. As seen from λ in the PPM region of figure 6, the width of the quantum oscillation increases as s/t increases. This is due to the interplay between the quantum nature of the phonon and the anharmonicity, and the increase of this width results in much stronger inter-electron attraction than in the harmonic case. Hence, u of the SDW is effectively reduced and erosion occurs.

Let us see the mixed case of a hard core and a soft one with $\gamma = 2.177$, $b = 0.642$ and $c = 0.07$, shown by the dotted lines in figure 5. When $u = 0$, the PPM region shrinks a little into a region with smaller s/t than the harmonic case, while in the large u/t region the PPM erodes the SDW region given by the harmonic case. This shrinkage of the PPM can be understood straight away from the dotted curve in figure 1. Because of the plateau-like region of $v(q_l)$, which is below the harmonic case, a large-amplitude Peierls distortion can occur more easily. On the other hand, the suppression of the SDW occurs for the same reason as that of the hard-core case.

6. Superconducting state

Let us now calculate T_c and its isotope shift. As mentioned before, our system is basically in the adiabatic situation, in the sense that the total electron bandwidth is much greater than the phonon energy $\hbar\omega_0$. In such a case, because of Migdal's theorem, the formation of BCS-type pairing order results in only a small energy lowering from the PPM state as compared with $\hbar\omega_0$. Consequently, even if we have taken the pairing order into account, the phase diagram shown in figure 5 is almost unaltered, except that a part of the PPM region changes to the SP region.

For this reason, in this section, we estimate T_c using the results obtained for the PPM state in section 4. First we transform h by M_m given by equations (4.1) and (4.7), which, as mentioned before, generates the moving lattice distortion and also transforms the bare electron into the polaron. Except for unimportant constant terms, h, is transformed as

$$M_m^{-1} h M_m = -\sum_{l,l',\sigma} t(l-l') a_{l\sigma}^{+} a_{l'\sigma} X(p_l, p_{l'}) - \sum_{l} [sY(q_l) - u](n_{l\alpha} - \bar{n})(n_{l\beta} - \bar{n})$$
$$- s^{1/2} \sum_{l,\sigma} W(q_l)(n_{l\sigma} - \bar{n}) + h_p'. \tag{6.1}$$

Similar to equation (4.3), the first term is the transfer of a polaron, and $X(p_l, p_{l'})$ denotes an operator that describes the overlap of the phonon clouds at sites l and l'. It is given by

$$X(p_l, p_{l'}) \equiv \exp[-\mathrm{i}s^{1/2} q(p_l - p_{l'})]. \tag{6.2}$$

The second term denotes the effective inter-polaron interaction, which includes both

the coulombic repulsion u and the attraction mediated by the phonon clouds. The operator $Y(q_l)$ denotes this phonon-mediated part and is given as

$$Y(q_l) \equiv q[2 - \gamma q + bq(6q_l^2 + sq^2) - cq(15q_l^4 + 15q_l^2 sq^2 + s^2q^4)] \tag{6.3}$$

where the second, third and fourth terms in the square brackets denote the increase of the potential energy of the lattice to create the phonon cloud around the electron. They contribute to reducing the attraction. The third term of equation (6.1) denotes the coupling between the polaron and the anharmonicity phonon, whose equilibrium position has already been displaced by the transformation M_m. Here $W(q_l)$ is the non-linear operator of q_l defined as

$$W(q_l) \equiv q_l[1 - \gamma q + 2bq(q_l^2 + sq^2) - cq(3q_l^4 + 10q_l^2 sq^2 + 3s^2q^4)]. \tag{6.4}$$

The fourth term h_p' is the Hamiltonian of the anharmonic phonons and is given as

$$h_p' \equiv \sum_l \left(\frac{p_l^2}{2(1+\Delta)} + v'(q_l) \right)$$

with

$$v'(q_l) \equiv \tfrac{1}{2}\gamma q q_l^2 - \tfrac{1}{2}bq_l^2(q_l^2 + 3sq^2) + \tfrac{1}{4}cq_l^2[2q_l^4 + 15sq^2(q_l^2 + sq^2)]. \tag{6.5}$$

We should note that this h_p' is almost the same as the fourth term of equation (2.5), and $W(q_l)$ in equation (6.4) is also not very much different from q_l, since b, c and q are of the order of one-tenth.

In the theories for the CDW, PPM and SDW states developed in previous sections, we have used the scaling transformation M_s to determine the phonon. This is basically a harmonic approximation, although the width of the quantum oscillation is determined variationally, so as to take the effect of the sextic anharmonicity into account. The purpose of this approximation is to determine only the relative stability between the aforementioned three states within the framework of the mean-field theory.

To determine isotope shifts of T_c as a function of the anharmonicity, however, this harmonic approximation is insufficient. As explained in section 2 in detail, the isotope shift is very sensitive to the nature of the ground- and the excited-state wavefunctions of the lattice vibration.

For this reason, in the present section, we use a more precise method. The jth eigenvalue ($\equiv \varepsilon_j'(\Delta, \gamma, b, c)$) of h_p' and its eigenfunction ($\equiv |jl(\Delta, \gamma, b, c)\rangle'$) at site l can be determined by the following equation:

$$(p_l^2/2(1+\Delta) + v'(q_l))\,|jl(\Delta,\gamma,b,c)\rangle' = \varepsilon_j'(\Delta,\gamma,b,c)\,|jl(\Delta,\gamma,b,c)\rangle' \qquad j = 0, 1, 2, \ldots \tag{6.6}$$

and using this eigenstate, we approximate X and Y in equation (6.1) by their averages as

$$\begin{aligned} X &\to x \equiv \mathrm{Tr}(\mathrm{e}^{-\theta h_p'} X)/\mathrm{Tr}(\mathrm{e}^{-\theta h_p'}) \\ Y &\to y \equiv \mathrm{Tr}(\mathrm{e}^{-\theta h_p'} Y)/\mathrm{Tr}(\mathrm{e}^{-\theta h_p'}). \end{aligned} \tag{6.7}$$

We are now in the position to transform the electrons into the Nambu formalism as

$$a_{l\alpha} \to A_{l1} \qquad a_{l\beta}^{+} \to A_{l2}$$

and our Hamiltonian can be rewritten as a new Hamiltonian h_{sp} except for constant terms

$$M_m^{-1} h M_m \to h_{sp}$$

which is given as

$$h_{sp} \equiv h_0 + h_p' + h_i. \tag{6.8}$$

Here, h_0 comes from the first term of equation (6.1) and is defined as

$$\begin{aligned} h_0 &\equiv \sum_k e'(k)(A_{k1}^\dagger A_{k1} - A_{k2}^\dagger A_{k2}) \qquad e'(k) \equiv -x(e(k)-\mu) \\ A_{ki} &\equiv \sum_l N^{-1/2}\, e^{-ik\cdot l} A_{li} \end{aligned} \tag{6.9}$$

and h_i denotes the interactions

$$h_i \equiv (sy-u)\sum_l (A_{l1}^\dagger A_{l1} - \bar{n})(A_{l2}^\dagger A_{l2} - \bar{n}) - s^{1/2}\sum_l W(q_l)\,(A_{l1}^\dagger A_{l1} - A_{l2}^\dagger A_{l2}). \tag{6.10}$$

Using this h_{sp}, we now calculate the one-particle Green function $\mathcal{G}(\tau-\tau')$. It has two time variables τ and τ', and has a $2N \times 2N$ matrix form in the Hilbert space spanned by the Wannier functions of the electron ($\equiv|li\rangle$), ($i = 1, 2$), with up ($i = 1$) and down ($i = 2$) spins at each site l. Its element can be defined as

$$\begin{aligned} (ki|\mathcal{G}(\tau-\tau')|k'i') &\equiv -\,\mathrm{Tr}\{e^{-\theta h_{sp}} T_+ [A_{ki}(\tau) A_{k'i'}^\dagger(\tau')]\}/\mathrm{Tr}(e^{-\theta h_{sp}}) \\ |ki) &\equiv \sum_l N^{-1/2}\, e^{ik\cdot l}|li) \end{aligned}$$

where T_+ is the time ordering operator, and the time evolution of an operator O is given as

$$O(\tau) \equiv e^{\tau h_{sp}} O\, e^{-\tau h_{sp}}.$$

Since we are mainly interested in the isotope shift of T_c due to the anharmonicity, we hereafter restrict ourselves to the small u region. In the large u region, as shown by Morel *et al*, the isotope shift is somewhat reduced by u even in the harmonic case [15]. According to the conventional BCS theory, we expand the Green function with respect to h_i as

$$\begin{aligned} (ki|\mathcal{G}(\tau-\tau')|k'i') &= (ki|\mathcal{G}_0(\tau-\tau')|k'i') \\ &+ \sum_l \int_0^\theta d\tau_1 (ki|\mathcal{G}_0(\tau-\tau_1)|li)(li'|\mathcal{G}_0(\tau_1-\tau')|k'i') \\ &\times [-(sy-u)(1-\delta_{ii'})(li|\mathcal{G}(-0)|li')] \\ &+ \sum_l \int_0^\theta d\tau_1 \int_0^\theta d\tau_2 (ki|\mathcal{G}_0(\tau-\tau_2)|li)(li'|\mathcal{G}_0(\tau_1-\tau')|k'i') \\ &\times [-s(1-\delta_{ii'})(li|\mathcal{G}(\tau_2-\tau_1)|li')D(\tau_2-\tau_1)] + \ldots \end{aligned} \tag{6.11}$$

wherein the time evolution of an operator O is now given as

$$O(\tau) = \mathrm{e}^{\tau(h_0+h'_{\mathrm{p}})} O\, \mathrm{e}^{-\tau(h_0+h'_{\mathrm{p}})}$$

and $\mathcal{G}_0(\tau - \tau')$ denotes the Green function given only by h_0, while $D(\tau - \tau')$ is the Green function of the anharmonic phonon,

$$D(\tau_2 - \tau_1) \equiv \mathrm{Tr}\{\mathrm{e}^{-\theta h'_{\mathrm{p}}} T_+ [W(q_l(\tau_2))W(q_l(\tau_1))]\}/\mathrm{Tr}(\mathrm{e}^{-\theta h'_{\mathrm{p}}}). \tag{6.12}$$

Since the region of temperature relevant to T_c is small, $k_B T_c \ll \hbar\omega_0$, we can simplify this Green function within the lowest two vibronic states as

$$D(\tau_2 - \tau_1) \rightarrow \sum_l N^{-1} |\langle 1l|W(q_l)|0l\rangle'|^2 \, \mathrm{e}^{-\varepsilon'_{10}|\tau_2 - \tau_1|} \tag{6.13}$$

$$\varepsilon'_{10} \equiv \varepsilon'_1 - \varepsilon'_0. \tag{6.14}$$

In the above expansion for $\mathcal{G}(\tau - \tau')$, we have taken into account only the off-diagonal part of the interaction and the diagonal part is neglected, since the polaron effect has already been included in h_0. As for higher-order terms not written explicitly in equation (6.11), we take only the diagrams that are reducible into these lowest two terms.

Taking the Fourier component of equation (6.11) with frequency ω_m,

$$\omega_m \equiv \pi(2m + 1)/\theta \qquad m = 0, \pm 1, \pm 2, \ldots \tag{6.15}$$

we can get the Green function ($\equiv \mathcal{G}(\mathrm{i}\omega_m)$) based on the BCS-type mean-field theory instead of the exact one. It is given as

$$\mathcal{G}(\mathrm{i}\omega_m) = [\mathrm{i}\omega_m - \hbar_0 - \mathcal{F}(\mathrm{i}\omega_m)]^{-1} \tag{6.16}$$

where $\hbar_0$ is the one-electron version of h_0

$$\hbar_0 \equiv \sum_k e'(k)[|k1)(k1| - |k2)(k2|] \tag{6.17}$$

and $\mathcal{F}(\mathrm{i}\omega_m)$ denotes the off-diagonal self-energy, coming from h_i, and is defined as

$$\mathcal{F}(\mathrm{i}\omega_m) \equiv \sum_{l,i,i'} \{|li)(1 - \delta_{ii'})[F^{\mathrm{A}}_{ii'}(\mathrm{i}\omega_m) + F^{\mathrm{B}}_{ii'}(\mathrm{i}\omega_m)](li'|\}. \tag{6.18}$$

$F^{\mathrm{A}}_{ii'}$ comes from the second term of equation (6.11) and is given as

$$F^{\mathrm{A}}_{ii'}(\mathrm{i}\omega_m) \equiv -(sy - u)\theta^{-1} N^{-1} \sum_{l,m'} \mathrm{e}^{+\mathrm{i}\omega_{m'}0} (li|\mathcal{G}(\mathrm{i}\omega_{m'})|li') \tag{6.19}$$

while $F^{\mathrm{B}}_{ii'}$ comes from the third term of equation (6.11), and is given as

$$F^{\mathrm{B}}_{ii'}(\mathrm{i}\omega_m) \equiv -s\theta^{-1} N^{-1} \sum_{l,m'} D(\mathrm{i}\nu_{m-m'})(li|\mathcal{G}(\mathrm{i}\omega_{m'})|li'). \tag{6.20}$$

Here, $D(\mathrm{i}\nu_m)$ is the Fourier component of $D(\tau)$ given by equation (6.13), and becomes

$$D(\mathrm{i}\nu_m) = \sum_l N^{-1} |\langle 1l|W(q_l)|0l\rangle'|^2 \left(\frac{1}{\varepsilon'_{10} + \mathrm{i}\nu_m} + \frac{1}{\varepsilon'_{10} - \mathrm{i}\nu_m}\right) \qquad \nu_m \equiv 2\pi m/\theta.$$

In order to perform the summation over m in equations (6.19) and (6.20), we define the imaginary part of the off-diagonal element as

$$\rho_{ii'}(E) \equiv -\pi^{-1}\,\mathrm{Im}[(li|\mathcal{G}(E+\mathrm{i}\varepsilon)|li')] \tag{6.21}$$

and in terms of it, we can formally rewrite $\mathcal{G}(\mathrm{i}\omega_m)$ as

$$(li|\mathcal{G}(\mathrm{i}\omega_m)|li') = \int \mathrm{d}E'\,\frac{\rho_{ii'}(E')}{\mathrm{i}\omega_m - E'}. \tag{6.22}$$

We substitute this new form into equations (6.19) and (6.20), and get

$$F^{\mathrm{A}}_{ii'} = -(sy-u)\int \mathrm{d}E'\,\rho_{ii'}(E')n(E') \tag{6.23}$$

$$F^{\mathrm{B}}_{ii'}(E+\mathrm{i}\varepsilon) = -s\sum_l N^{-1}\,|\langle 1l|W(q_l)|0l\rangle'|^2 \times \int \mathrm{d}E'\rho_{ii'}(E')\left(\frac{1-n(E')}{E+\mathrm{i}\varepsilon-(E'+\varepsilon'_{10})}+\frac{n(E')}{E+\mathrm{i}\varepsilon-(E'-\varepsilon'_{10})}\right) \tag{6.24}$$

which are essentially the same as the Eliashberg equation for the system with an anharmonic phonon. In practical calculations we use the following form for the off-diagonal part:

$$(li|\mathcal{G}(E+\mathrm{i}\varepsilon)|li') = \sum_k N^{-1}\,\frac{(F^{\mathrm{A}}_{ii'}+F^{\mathrm{B}}_{ii'})}{2I_k}\left(\frac{1}{E+\mathrm{i}\varepsilon-I_k}-\frac{1}{E+\mathrm{i}\varepsilon+I_k}\right) \tag{6.25}$$

$$I_k \equiv \{[e'(k)]^2+(F^{\mathrm{A}}_{12}+F^{\mathrm{B}}_{12})(F^{\mathrm{A}}_{21}+F^{\mathrm{B}}_{21})\}^{1/2}.$$

Using this theoretical framework, let us now discuss the essential nature of T_c of this system and its isotope shift. As one of the typical cases for isotopic substitution, we now set Δ at $\Delta = 0.125$, which corresponds to the case of $^{16}\mathrm{O} \rightarrow {}^{18}\mathrm{O}$ substitution in transition-metal oxides. In this case, $\varepsilon_{10}(0.125, \gamma, b, c)$ decreases by about 6% from $\varepsilon_{10}(0, \gamma, b, c)$ as seen from figures 2 and 3. The relative change ($\equiv r$) of F_{eff} in equation (2.10) due to this substitution is given as

$$r \equiv \frac{|\langle 1l(0.125,\gamma,b,c)|q_l|0l(0.125,\gamma,b,c)\rangle|^2/\varepsilon_{10}(0.125,\gamma,b,c)}{|\langle 1l(0,\gamma,b,c)|q_l|0l(0,\gamma,b,c)\rangle|^2/\varepsilon_{10}(0,\gamma,b,c)} \tag{6.26}$$

and this r is also shown in figures 2 and 3 as a function of c.

In the hard-core type anharmonic case, we can see from figure 2 that r increases from 1 as c increases. Although this increase of r is small, it is enough to cancel the aforementioned decrease of ε_{10}, since the change of r is enhanced by s as seen from equation (2.10).

Keeping this qualitative nature of the isotope shift in mind, we have solved the aforementioned equations for T_c in detail within the BCS theory. Since T_c takes its maximum value at the phase boundary, only these boundary regions for given anharmonicities are shown in figure 7.

We can see from case (b) of figure 7 that the isotope shift disappears when $b = 0$ and $c = 0.03$. We can also see that the maximum value of T_c itself increases as c increases from the harmonic case, because the boundary between the PPM and the CDW also shifts to the stronger region of s. As mentioned at the beginning, t and $\hbar\omega_0$ are fixed at $t = 3.125$ and $\hbar\omega_0 = 0.08$ eV. In this case, T_c amounts to about $50 \sim 100$ K.

When this hard-core type anharmonicity becomes stronger, the maximum value of T_c increases further, and we get a negative isotope shift as shown in case (d) in figure 7.

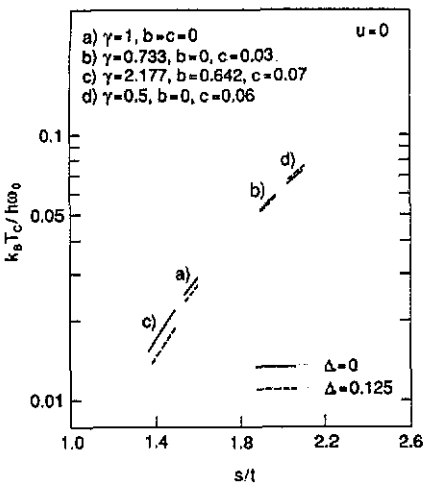

Figure 7. Plot of $k_BT_c/\hbar\omega_0$ as a function of s/t, Δ, γ, b and c, for $u = 0, t = 3.125$: (——) $\Delta = 0$; (– – – –) $\Delta = 0.125$.

On the other hand, in the case of mixed type anharmonicity, we can see from figure 3 that r decreases from 1 as c increases. Thus, we get a strongly enhanced isotope shift. When $b = 0.642$ and $c = 0.07$, the relative shift of T_c becomes twice as big as that of the harmonic case, as shown in case (c) of figure 7. As for the value of T_c itself, its maximum decreases from that of the harmonic case because the SP state is suppressed by the CDW, as mentioned in section 5.

7. Conclusion and discussion

Thus, we have been concerned with the anharmonic Peierls–Hubbard model, and calculated the phase diagram, metal–insulator transitions, T_c and its isotope shifts. In the case of the hard-core type anharmonicity, the metal–insulator transition is greatly suppressed, and the system remains metallic even when the e–ph coupling is very strong. This metallic state falls into the SP state at high enough T_c of about $50 \sim 100$ K, with no isotope effect. In the case of the mixed type anharmonicity between the hard core and the soft one, on the other hand, T_c is suppressed by the occurrence of the CDW, and its relative isotope shift becomes about twice as great as that of the harmonic case. In both these two anharmonic cases, the transition from the metallic state to the SDW state is always suppressed.

From these results, we can conclude that there are various types of isotope shifts, enhanced ones, very small ones and even negative ones. We can also conclude that the height of T_c, its isotope shift and the instabilities of the SP state itself are all closely related with each other through the anharmonicity. Hence, none of them can be considered separately.

How to observe this local anharmonicity has been considered in detail in our previous paper [16]. Problems related to the microscopic origin of the anharmonicity are our theme of future studies.

The metal–insulator transitions shown in figure 5 are only due to the competition between T, S, U and the anharmonicity, under the condition that the total number of electrons does not change and always keeps the half-filled case. In connection with Cu–O type compounds, however, it is already well known that the transition from an

insulator to a metal occurs only by doping, that is, only by decreasing the total number of electrons. Our studies for this doping effect are postponed to the future.

Acknowledgment

This work is supported by the Grant-in-Aid for Science Research on New Functionalized Materials from Ministry of Education, Science and Culture of Japan (no 03204006).

References

[1] Nasu K 1987 *Phys. Rev.* B **35** 1748
[2] Nasu K and Toyozawa Y 1982 *J. Phys. Soc. Japan* **51** 2098
[3] Drechsler S and Plakida N 1987 *Phys. Status Solidi* **144** K113
[4] Muller K 1990 *Z. Phys.* B **80** 193
[5] Feile R, Leiderer P, Kowalewski J, Assmus W, Schubert J and Poppe U 1988 *Z. Phys.* B **73** 155
[6] Genzel L, Wittlin A, Bauer M, Cardona M, Schonherr E and Simon A 1989 *Phys. Rev.* B **40** 2170
[7] Sugai S 1989 *Phys. Rev.* B **39** 4306
[8] Foster C, Heeger A, Kim Y, Stuky G and Herron N 1989 *Physica* C **162–164** 1107
[9] Taliani C, Pal A, Ruani G, Zamboni R, Wei X and Vardeny Z 1990 *Electronic Properties of High T_c Superconductors and Related Compounds* ed H Kuzmany, M Mehring and J Fink (Berlin: Springer) preprint
[10] Huang Q, Zasadzinski J, Tralshawala N, Gray K, Hinks D, Peng J and Greene R 1990 *Nature* **347** 369
[11] Shimada D, Miyakawa N, Kido T and Tuda N 1989 *J. Phys. Soc. Japan* **58** 387
[12] Crawford M, Farneth W, McCarron E, Harlow R and Moudden A 1990 *Science* **250** 1390
[13] Sera M, Ando Y, Kondoh S, Fukuda K, Sato M, Watanabe I and Kumagai K 1989 *Solid State Commun.* **69** 851
[14] Maeno Y, Odagawa A, Kakehi N, Suzuki T and Fujita T 1991 *Physica* C **173** 322
[15] Morel P and Anderson P 1962 *Phys. Rev.* **125** 1263
[16] Nasu K 1991 *Phys. Rev.* B **44** 7625